The Astrophysical Journal, 647:552–557, 2006 August 10

AMMONIA AS A TRACER OF CHEMICAL EQUILIBRIUM IN THE T7.5 DWARF GLIESE 570D

D. Saumon,[1] M. S. Marley,[2] M. C. Cushing,[3,4] S. K. Leggett,[5] T. L. Roellig,[6] K. Lodders,[7] and R. S. Freedman[8]

Received 2006 March 15; accepted 2006 April 25

ABSTRACT

We present the first analysis of an optical to mid-infrared spectrum of the T7.5 dwarf Gliese 570D with model atmospheres, synthetic spectra, and brown dwarf evolution sequences. We obtain precise values for the basic parameters of Gl 570D: $T_{\rm eff} = 800$–820 K, $\log g$ (cm s^{-2}) $= 5.09$–5.23, and $\log (L/L_\odot) = -5.525$ to -5.551. The *Spitzer* Infrared Spectrograph (IRS) spectrum shows prominent features of ammonia (NH_3) that can only be fitted by reducing the abundance of NH_3 by about 1 order of magnitude from the value obtained with chemical-equilibrium models. We model departures from chemical equilibrium in the atmosphere of Gl 570D by considering the kinetics of nitrogen and carbon chemistry in the presence of vertical mixing. The resulting model spectrum reproduces the data very well.

Subject headings: stars: abundances — stars: atmospheres — stars: individual (Gliese 570D) — stars: low-mass, brown dwarfs

Online material: color figures

1. INTRODUCTION

Ammonia is the only significant nitrogen-bearing compound that can be readily observed in brown dwarfs. Its presence in very cool brown dwarf atmospheres has been expected for some time (Tsuji 1964; Marley et al. 1996; Fegley & Lodders 1996; Saumon et al. 2000, 2003; Allard et al. 2001; Lodders & Fegley 2002; Burrows et al. 2003). Saumon et al. (2000) reported a detection of weak NH_3 features in the near-infrared spectrum of the T7p dwarf Gl 229B, but a clear detection had to await the *Spitzer* Infrared Spectrograph (IRS) observation of the T1/T6 binary ϵ Indi Bab (Roellig et al. 2004). IRS spectra also reveal the presence of NH_3 in all observed dwarfs with spectral types of T2 and later (Cushing et al. 2006).

In addition to its importance as a strong absorber in very cool brown dwarfs, NH_3 provides an important window into the phenomenon of nonequilibrium chemistry. Because some chemical reactions proceed very slowly at the relatively low temperatures encountered in the atmospheres of T dwarfs, vertical transport can lead to chemical abundances that depart from local thermodynamic equilibrium. This phenomenon has long been established in Jovian planets (Barshay & Lewis 1978; Fegley & Prinn 1985; Fegley & Lodders 1994; Lodders & Fegley 1994). In brown dwarfs, the strongest expected signatures of departures from equilibrium chemistry are an overabundance of CO and depletion of NH_3. The prediction of nonequilibrium chemistry in brown dwarfs (Fegley & Lodders 1996) was quickly confirmed by the detection of the 4.7 μm band of CO in Gl 229B (Noll et al. 1997), and subsequently by the detection of NH_3 in a high-resolution near-IR spectrum (Saumon et al. 2000). Nonequilibrium chemistry may be common in cool brown dwarfs since M' photometry shows a systematic flux depletion in T6–T9 dwarfs that can be attributed to enhanced CO 4.7 μm absorption (Golimowski et al. 2004) relative to models in chemical equilibrium.

With a spectral type of T7.5, Gl 570D (Burgasser, et al. 2000; Burgasser et al. 2006) is one of the latest T dwarfs known, and its IRS spectrum shows the strongest 10–11 μm NH_3 absorption observed so far (Cushing et al. 2006). It is a particularly interesting target, since it is a wide companion to the well-studied K4 V star Gl 570A, and to a pair of M dwarfs, Gl 570BC. The distance, metallicity, and age of the system very effectively reduce the parameter space allowed to model Gl 570D. Geballe et al. (2001) used these constraints to determine the effective temperature $T_{\rm eff}$ and gravity g of Gl 570D and to analyze its optical and near-infrared spectrum. Here, we take advantage of the new spectroscopic information provided by the IRS spectrum to redetermine $T_{\rm eff}$ and g. We also perform the first quantitative analysis of the NH_3 10–11 μm band for any brown dwarf.

2. OBSERVATIONS AND DATA REDUCTION

Our analysis of Gl 570D is based on spectroscopic data covering most of its spectral energy distribution. We combine a Keck Low Resolution Imaging Spectrograph (LRIS) 0.63–1.01 μm optical spectrum (Burgasser et al. 2003) with a United Kingdom Infrared Telescope (UKIRT) CGS4 near-IR spectrum covering 0.79–1.35 μm and 1.43–2.52 μm (Geballe et al. 2001), and an IRS Short-Low module spectrum that covers 5.43–14.68 μm (Cushing et al. 2006). Absolute-flux calibration for the UKIRT and IRS spectra was obtained by using Mauna Kea Observatories (MKO) photometry (Leggett et al. 2002) and Infrared Array Camera (IRAC) band 4 photometry (Patten et al. 2006), respectively. The far-red optical spectrum was then scaled to match the flux density level of the flux-calibrated UKIRT spectrum.

3. MODELS: EVOLUTION AND SPECTRA

We analyze the spectrum of Gl 570D with a combination of model atmospheres, synthetic spectra, and evolution sequences. Its T7.5 spectral type strongly suggests that its atmosphere is free of condensates, and we use cloudless model atmospheres and synthetic

[1] Los Alamos National Laboratory, MS P365, Los Alamos, NM 87545; dsaumon@lanl.gov.
[2] NASA Ames Research Center, MS 245-3, Moffett Field, CA 94035-1000; mark.s.marley@nasa.gov.
[3] Steward Observatory, University of Arizona, 933 North Cherry Avenue, Tucson, AZ 85721; mcushing@as.arizona.edu.
[4] Spitzer Fellow.
[5] Joint Astronomy Center, University Park, Hilo, HI 96720; s.leggett@jach.hawaii.edu.
[6] NASA Ames Research Center, MS 245-6, Moffett Field, CA 94035-1000; thomas.l.roellig@nasa.gov.
[7] Department of Earth and Planetary Sciences, Washington University, Saint Louis, MO 63130-4899; lodders@levee.wustl.edu.
[8] SETI Institute, 515 North Wisham Road, Mountain View, CA 94043; freedman@darkstar.arc.nasa.gov.

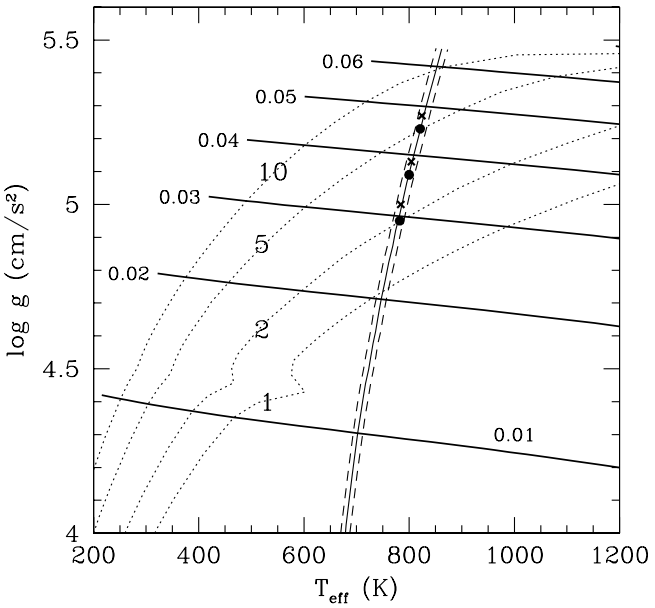

FIG. 1.— $T_{\rm eff}$ and gravity for Gl 570D. Our brown dwarf evolution tracks are shown by thick black lines labeled with the mass in $M_{\odot}$. Isochrones (*dotted lines*) are labeled in Gyr. The nearly vertical lines (*solid and dashed*) are the locus of $(T_{\rm eff}, g)$ points with $\log L/L_{\odot} = -5.525 \pm 0.024$. The circles show the three models of Table 1. For comparison, the crosses show the values obtained by Geballe et al. (2001). [*See the electronic edition of the Journal for a color version of this figure.*]

spectra that were most recently described in Fortney et al. (2006 and references therein). Averaging recent metallicity determinations for Gl 570A (Thorén & Feltzing 2000; Santos et al. 2005; Valenti & Fisher 2005) gives $[{\rm Fe/H}] = 0.09 \pm 0.04$. This slight enrichment is negligible in view of the other uncertainties in the data and models, and our entire analysis assumes solar metallicity (Lodders 2003).

We have developed an evolution code for brown dwarfs that assumes an adiabatic internal structure. It uses the H/He equation of state of Saumon et al. (1995). Nuclear energy generation through the first branch of the *p-p* chain (Burrows & Liebert 1993) is included. We use the Nuclear Astrophysics Compilation of Reaction (NACRE) rates (Angulo et al. 1999) and ion-ion and electron-ion screening factors (G. Chabrier 2005, private communication). The surface boundary condition is obtained from our atmosphere models. All brown dwarf atmosphere models become convective at depth, where the specific entropy of the gas becomes essentially constant. The value of the entropy at the bottom of the atmospheres $S_{\rm atm}$ gives the entropy for the adiabatic interior. The boundary condition is described as a tabulated function $S_{\rm atm}(T_{\rm eff}, g, [{\rm Fe/H}])$. Thus, our cooling sequences are fully consistent with the atmosphere models (Chabrier & Baraffe 1997). Details of the evolution calculation will be provided in a future publication.

4. DETERMINATION OF THE PHYSICAL PARAMETERS

We follow the method developed by Saumon et al. (2000) and initially applied to Gl 570D by Geballe et al. (2001). Briefly, we use the optical, near-IR, and mid-IR spectra to determine the integrated flux observed at Earth ($1.875 \pm 0.107 \times 10^{-12}$ ergs s^{-1} cm^{-2}).[9] This represents about 70% of the bolometric flux of Gl 570D. We use our grid of model spectra to compute the bolometric correction and the bolometric luminosity, $L^s_{\rm bol}(T_{\rm eff}, g)$, which depends on the yet-to-be-determined $T_{\rm eff}$ and g. An independent relation $L^e_{\rm bol}(T_{\rm eff}, g)$ is given by our evolution sequences. A consistent solution between the spectrum and the evolution is obtained by imposing $L^s_{\rm bol} = L^e_{\rm bol}$. This gives a family of solutions $T_{\rm eff}(g)$ (Fig. 1). A combination of age indicators shows that the Gl 570 system is between 2 and 5 Gyr old (Geballe et al. 2001), which constrains the range of the gravity to that shown by the isochrones in Figure 1 and the models in Table 1. Models A and C bracket the age limits, and model B corresponds to the midpoint. This new determination of the physical parameters of Gl 570D differs from that of Geballe et al. (2001) in several ways. The observed spectral energy distribution (SED) has been greatly extended by the *Spitzer* IRS spectrum, and the near-IR spectrum has been recalibrated using the latest MKO photometry. The atmosphere models have steadily improved, most notably with the inclusion of a more extensive line list for CH_4 (Champion et al. 1992; R. Freedman & K. Lodders 2006, in preparation). Finally, the evolution is computed with an independent code using our cloudless atmosphere grid as the surface boundary condition rather than relying on the sequences of Burrows et al. (1997). Despite all these changes, the parameters obtained for Gl 570D are remarkably similar to those of Geballe et al. (2001) (Fig. 1, *crosses*). Most of the difference can be attributed to a shift of the isochrones in the $(T_{\rm eff}, g)$ plane between our evolution sequences and those of Burrows et al. (1997) caused mainly by the different surface boundary conditions. This shows that the method is quite robust, and that further improvements in the models will not significantly affect the values in Table 1.

Figure 1 shows that the main uncertainty in the $T_{\rm eff}$ and g of Gl 570D arises from the uncertainty in the age of the system. By comparison, the uncertainty in $L_{\rm bol}$ from the flux calibration of the data is small.

Given $T_{\rm eff}$ and g, the radius $R(T_{\rm eff}, g)$ from the evolution, and the parallax of Gl 570A, we can compute model fluxes at Earth that can be compared directly to the data. The model B spectrum is shown in Figure 2. This is not a fit of the spectrum per se, but it is obtained solely from the procedure outlined above. The agreement with the optical and near-IR data is generally excellent. The deviations in the 1.6–1.7 μm region are due to the incomplete CH_4 line list. The reason for the underestimated *K*-band flux is unclear. Models computed with the slightly higher metallicity of Gl 570A would give a higher *K*-band flux. A similar effect could also be obtained by flux redistribution from a stronger CH_4 1.6 μm band computed from a more complete line list. We find that a cloudy model with a thin cloud deck parameterized by a sedimentation parameter $f_{\rm sed} = 4$ (Ackerman & Marley 2001) can also substantially improve the agreement with the observed *K*-band peak.

In the mid-IR, the model systematically underestimates the flux beyond 9 μm, which coincides with strong absorption by NH_3. The outlier models (A and C in Table 1) give very similar synthetic spectra. The differences remain below ± 0.03 mJy in the near-IR and $\pm$ 0.2 mJy in the mid-IR, with higher gravity models giving lower fluxes.

5. NONEQUILIBRIUM CHEMISTRY OF NH_3

Vertical transport in the atmosphere of a T dwarf will result in a reduced NH_3 abundance, which will increase the model flux for $\lambda \gtrsim 9$ μm and improve the agreement with the IRS spectrum. We consider atmosphere models that depart from chemical equilibrium to optimize the fit to the data.

The kinetics of the chemistry of carbon and nitrogen in giant planets and brown dwarfs has been described in detail in Lewis & Prinn (1980), Fegley & Lodders (1994), Griffith & Yelle (1999),

[9] The uncertainty estimate is obtained from the uncertainties in the absolute calibration of each piece of the SED (3% for the optical spectrum, 5% for the near-IR spectrum, and 6.5% for the IRS spectrum). A total uncertainty of $\pm$5.7% is based on conservatively assuming that the individual calibration uncertainties all add in the same direction. The 1% uncertainty on the distance (Perryman et al. 1997) is negligible by comparison.

TABLE 1
Range of Physical Parameters of Gliese 570D

Model	$T_{\rm eff}$ (K)	log g (cm s^{-2})	log($L/L_\odot$)	Mass ($M_{\rm J}$)	Radius ($R_\odot$)	Age (Gyr)
A.....	782	4.95	−5.503	31	0.0950	2.0
B.....	800	5.09	−5.525	38	0.0901	3.2
C.....	821	5.23	−5.551	47	0.0853	5.0

Lodders & Fegley (2002, 2006), and Bézard et al. (2002), and the effect on the spectra of brown dwarfs has been described in Saumon et al. (2003). We only provide a brief summary of nonequilibrium chemistry here.

5.1. *Nonequilibrium Carbon and Nitrogen Chemistry*

The chemistry of carbon and nitrogen in brown dwarf atmospheres is essentially described by the net reactions

$$\mathrm{CO} + 3\mathrm{H_2} \leftrightarrow \mathrm{CH_4} + \mathrm{H_2O}, \quad (1)$$

$$\mathrm{N_2} + 3\mathrm{H_2} \leftrightarrow 2\mathrm{NH_3}. \quad (2)$$

Because of the large binding energies of CO and N_2, both reactions proceed much more slowly to the right than to the left. Vertical mixing dredges up hot gas that is relatively rich in CO and N_2 to the cooler part of the atmosphere, where CO and N_2 are converted very slowly into CH_4 and NH_3, respectively. The net result is a relative overabundance of CO and N_2, and decreased abundances of CH_4 and NH_3, in the upper atmosphere. The abundance of H_2O is also reduced by conservation of the total number of oxygen atoms.

The correct chemical pathway and reaction timescale for the conversion of CO into CH_4 remains uncertain (Yung et al. 1988; Griffith & Yelle 1999; Bézard et al. 2002; Lodders & Fegley 2002; Visscher & Fegley 2005). We adopt the "fast" chemical timescale of Yung et al. (1988). For the N_2 conversion, we adopt the timescale given in Lodders & Fegley (2002).

5.2. *Vertical Transport*

Slow mixing can occur in the radiative zones of atmospheres through a variety of processes such as the turbulent decay of waves propagated upward from the convective/radiative boundary and instabilities arising from rapid rotation. In the absence of any detailed modeling of these processes, we adopt a simple model of vertical mixing by eddy turbulence (Griffith & Yelle 1999). This process is analogous to diffusion and occurs over a characteristic timescale $\tau_{\rm mix} \sim H^2/K$, where H is the pressure scale height and K is the coefficient of eddy diffusion; K ranges from $\sim 10^2$ to 10^5 cm^2 s^{-1} in planetary stratospheres, and it is the only free parameter in our nonequilibrium models.

The timescale for mixing in the atmospheric convection zone is $\tau_{\rm conv} \sim H_c/v_c$, where H_c and v_c are the convective mixing length and velocity, respectively, and are evaluated with the mixing length theory. For convenience, we choose $H_c = H$. Note that $\tau_{\rm conv} \ll \tau_{\rm mix}$.

5.3. *Quenching of the Chemistry*

The chemical-abundance profiles (Lodders & Fegley 2002) in model atmosphere B are shown in Figure 3. Depth in the atmosphere is indicated by the local temperature. The equilibrium abundances are shown with dashed lines that overlap solid lines for H_2O and CH_4. The transition in the carbon chemistry from CO deep in the atmosphere to CH_4 near the surface occurs at $\log T \sim 3.25$. The N_2 to NH_3 transition occurs around $\log T \sim 2.9$. Remarkably, and in contrast to the carbon chemistry, the N_2/NH_3 equilibrium ratio remains nearly constant deep in the atmosphere due to a near cancellation of the effects of the increased temperature (favoring N_2) and of the increased pressure (favoring NH_3) along this portion of the atmosphere profile.

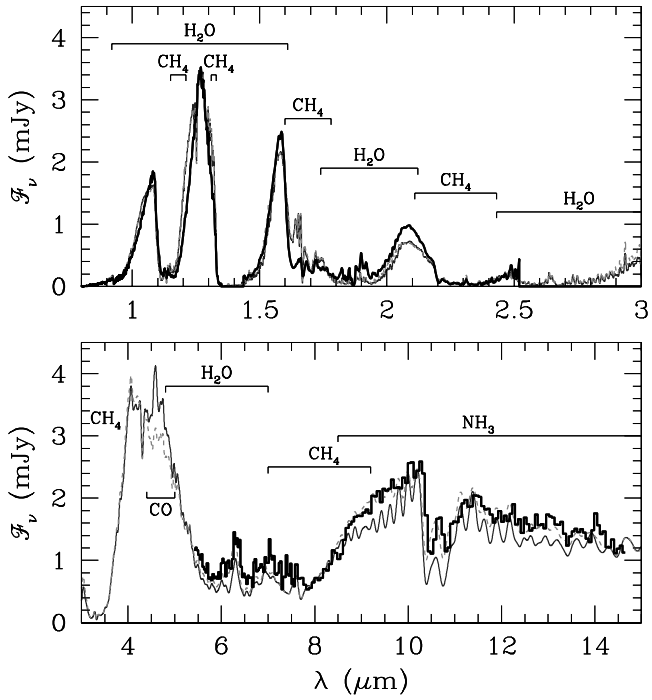

Fig. 2.—Comparison of the observed and modeled SED of Gl 570D. The data (*thick black curve and histogram*) are from Burgasser et al. (2003), Geballe et al. (2001), and Cushing et al. (2006). The equilibrium model B (Table 1) is shown by the thin solid line, and the best fitting nonequilibrium model (model C with $\log K = 2$) is shown by the dashed line. The main molecular absorbers are indicated. The models are plotted at a spectral resolution of $R = 500$ (*top*) and $R = 100$ (*bottom*), approximating the resolution of the data. [*See the electronic edition of the Journal for a color version of this figure.*]

The chemical timescales for the conversion of CO and N_2 are shown by the thick solid and dotted lines, respectively. These vary over more than 20 orders of magnitude throughout the atmosphere and become extremely long in the upper atmosphere. Mixing occurs rapidly in the convection zone, but it is about 7 orders of magnitude slower in the radiative zone for our choice of $K = 100$ cm^2 s^{-1}. In regions where $\tau_{\rm chem} < \tau_{\rm mix}$, chemical equilibrium prevails. Where $\tau_{\rm chem} > \tau_{\rm mix}$, however, abundances of CO, CH_4, N_2, NH_3, and H_2O will depart from equilibrium (*solid lines*). The nonequilibrium mole fractions are approximately determined by their values at which $\tau_{\rm chem} = \tau_{\rm mix}$. In our calculation, we adopt the scheme of Smith (1998) to determine this "quenching level." As can be seen in Figure 3, there can be more than one level where $\tau_{\rm chem} = \tau_{\rm mix}$, resulting in alternating zones in and out of chemical equilibrium. For simplicity, we consider only the uppermost (lowest T) crossing. It turns out that in all cases, this is an excellent approximation to the full solution for the chemical profile, since the deeper quenching occurs well below the level of formation of the corresponding molecular bands.

Figure 3 shows that above the CO quenching level ($\log T \sim 3.03$), the nonequilibrium abundance of CO is orders of magnitude higher than at equilibrium. The abundances of CH_4 and H_2O are barely affected for this choice of K (slow mixing). The NH_3 abundance is reduced by about 1 order of magnitude in the upper atmosphere. In this model, N_2 is quenched below the bottom of the atmosphere model in a region where N_2/NH_3 is still nearly

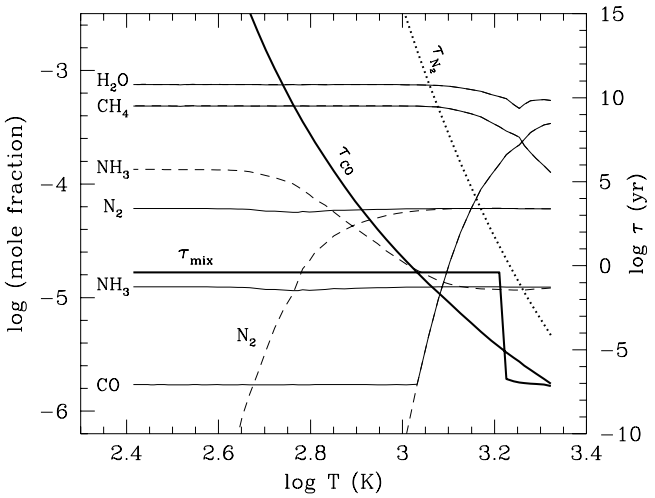

FIG. 3.— Chemical profile of model atmosphere B (Table 1). Mole fractions of H_2O, CH_4, N_2, NH_3, and CO are shown in equilibrium (*dashed curves*) and out of equilibrium ($\log K = 2$, *solid curves*) as a function of the temperature in the model atmosphere. The pressure increases from the top of the atmosphere (*left*) toward the bottom (*right*). Thick black lines show the mixing timescale ($\tau_{\rm mix}$) and the timescale for the destruction of CO ($\tau_{\rm CO}$, *solid line*) and N_2 (τ_{N_2}, *dotted line*). Timescales are given on the right axis. The mixing timescale is nearly discontinuous where the atmosphere becomes convective ($\log T \gtrsim 3.2$). The 10–11 μm NH_3 band is formed in the $\log T = 2.65$–2.9 region. [*See the electronic edition of the Journal for a color version of this figure.*]

constant. The fact that the equilibrium mole fraction of NH_3 is nearly constant for $\log T \gtrsim 3.1$ implies that the nonequilibrium NH_3 abundance profile is completely insensitive to the choice of the eddy mixing coefficient K over a very wide range ($\log K \gtrsim -8$). This means that *all* plausible choices of K will give the same NH_3 abundance and therefore the same mid-IR spectrum.

5.4. *Optimal Model*

In view of the above remarks, we arbitrarily choose $K = 100$ cm^2 s^{-1} to compute nonequilibrium spectra for the three models in Table 1. Besides the choice of equilibrium or nonequilibrium chemistry, the only fitting parameter left is the gravity, constrained to be between the values for models A and C (Table 1). We determine the goodness of fit of a synthetic spectrum by computing the χ^2 between the model and the data for $\lambda \geq 9$ μm, which is where NH_3 features are seen in the spectrum (Fig. 2). For this purpose, model spectra are smoothed to the IRS Short-Low point-source spectral resolution of $\lambda/\Delta\lambda = 126$ with a Gaussian filter and then binned to the instrument's wavelength sampling. The uncertainty (σ) in the fitted χ^2 is obtained by fitting 5000 simulated data sets generated by adding a random Gaussian noise distribution to each pixel with a width given by the individual pixel noise ($\sim$0.1 mJy). We also fit renormalized spectra to account for the $\pm$6.5% calibration uncertainty, which turns out to be the dominant source of uncertainty. Nonequilibrium model C always gives the best fit. A reasonable fit (2.8 σ worse than model C) is obtained with nonequilibrium model B if the observed flux is increased by the full 6.5% uncertainty. The best equilibrium-model fit is 6.7 σ worse than the best nonequilibrium-model fit.

The nonequilibrium model C spectrum is shown by the dashed curve in Figure 2. The agreement with the data is remarkable considering that all we have done is include nonequilibrium chemistry in the calculation and increase the gravity slightly, with no other free parameter. We conclude that the NH_3 abundance is reduced by nonequilibrium chemistry and that the parameters of Gl 570D fall between models B and C, and very likely closer to the latter.

6. ALTERNATIVE EXPLANATIONS FOR THE NH_3 DEPLETION

We briefly consider five possible explanations that could account for the enhanced mid-IR flux in Gl 570D: (1) a low nitrogen abundance, (2) an error in the temperature profile of the atmosphere, (3) uncertain NH_3 opacity, (4) time variability, and (5) photodissociation of NH_3.

6.1. *Low Nitrogen Abundance*

The metallicity of Gl 570D is very nearly solar based on abundance determinations of Na, Si, Ca, Ti, V, Cr, Fe, Co, and Ni in Gl 570A that range from $[{\rm X/H}] = -0.10$ to 0.24, with a typical spread of $\sim$0.1 between independent determinations (Santos et al. 2005; Thorén & Feltzing 2000; Valenti & Fisher 2005). To the best of our knowledge, however, the N abundance has not been measured. A low [N/H] value would result in a decreased NH_3 abundance that could potentially explain the relatively high mid-IR flux. The dependence of the mole fraction of ammonia on the nitrogen abundance is $\log X_{\rm NH_3} \sim 0.5[{\rm N/H}]$ (Lodders & Fegley 2002). In our models, the strongest NH_3 absorption occurs at a depth of $\log T = 2.65$ in the atmosphere, where the nonequilibrium chemistry reduces $X_{\rm NH_3}$ by a factor of 10 (Fig. 3). To obtain a similar reduction from a low nitrogen abundance would require $[{\rm N/H}] = -2$, which would be an extreme departure from the abundances of other metals in Gl 570A.

In principle, N-bearing condensates may also cause a depletion of N-bearing gases in the atmosphere. However, there are no N-bearing condensates expected along the (T,P) profile of Gl 570D that can significantly remove nitrogen, and temperatures are not low enough to allow NH_4SH or NH_3 condensation as in the much cooler upper atmospheres of the Jovian planets.

6.2. *Uncertainties in the Temperature Profile of the Atmosphere*

Our determination of $L_{\rm bol}$ and our solution for $T_{\rm eff}$ and g are in excellent agreement with the values obtained by Geballe et al. (2001) without the benefit of the IRS spectrum. This indicates that while the near-IR flux has remained constant, the unknown mid-IR flux of Gl 570D in 2000 March could not be significantly different from that measured in 2005 February. The fact that our equilibrium model is in very good agreement with the full SED of Gl 570D (Fig. 2) supports the notion that all pieces of the SED are consistent with each other. Finally, $T_{\rm eff}$ would have to increase to $\sim$1050 K to obtain an equilibrium NH_3 mole fraction similar to the nonequilibrium value needed to fit the IRS spectrum. Such a high $T_{\rm eff}$ is completely incompatible with *all* of the Gl 570D observations. If we consider the temperature profile of the atmosphere, an increase of over 200 K ($\sim$40%) at $P \lesssim 1$ bar would be required, an implausible error in our models and inconsistent with the near-IR spectrum of Gl 570D.

6.3. *Uncertainties in the* NH_3 *Opacity*

The opacity of NH_3 is computed from a line list obtained by combining the GEISA (Husson et al. 1992) and HITRAN (Rothman et al. 2005) databases, complemented with recent laboratory measurements and theoretical calculations (see Burrows et al. 1997 for more details). To our knowledge, this compilation of NH_3 opacity is the most complete currently available. Nonetheless, the line list is only complete up to $T = 300$ K, and transitions arising from levels that are excited only at higher temperatures are underrepresented or missing. Qualitatively, the NH_3 opacity we calculate for Gl 570D is a lower limit to the actual opacity,

implying that the derived underabundance of NH_3 is an *upper* limit. More quantitatively, the 9–14 μm band of NH_3 arises from the ground state ($\nu_0 \rightarrow \nu_2$), with a small overlapping contribution from the ν_2 excited state ($\nu_2 \rightarrow 2\nu_2$). The energy differences between other excited vibrational states of NH_3 are too large for the corresponding hot bands to overlap with the $\nu_0 \rightarrow \nu_2$ band. We are confident that the line list for the 9–14 μm band on which our analysis of the abundance of NH_3 is based is quite complete.

6.4. *Time Variability of Gl 570D*

The spectroscopic data analyzed here were gathered over a period of several years. The optical spectrum is from observations taken in 2000 March and 2001 February (Burgasser et al. 2003), the near-IR spectrum in 2000 March (Geballe et al. 2001), and the *Spitzer* IRS spectrum in 2005 February (Cushing et al. 2006). It is conceivable that the luminosity of Gl 570D may have varied during this 5 year period, affecting our determination of $T_{\rm eff}$ and g and fortuitously resulting in our excellent fit of the combined spectrum with a model departing from chemical equilibrium. Burgasser et al. (2003) do not report any variation in the optical flux of Gl 570D between their two observations taken one year apart, and the reported equivalent width of Cs I and Rb I lines shows no variation within 1.5 σ. The near-IR spectrum is calibrated to *JHK* MKO photometry taken in 2000 February (Geballe et al. 2001). Repeat observations in 2005 July are fully consistent (<1 σ) with the original photometry. The Two Micron All Sky Survey (2MASS) photometry of Gl 570D was obtained in 1998 May and 1999 July. Burgasser (2002) reports a change of 0.26 mag in J between the two epochs and no significant change in H or K_s. However, the variation in J magnitude is within the scatter of 2MASS photometry between the two epochs for objects in the field of Gl 570D of similar J magnitude. Applying the color transformation of Stephens & Leggett (2004) to the first epoch 2MASS photometry shows agreement to 2 σ (J), 1 σ (H), and <1 σ (K) with the MKO magnitudes. Based primarily on the stability of the near-IR MKO photometry, we conclude that any time variability in Gl 570D over a period of 7 years is at most at the 2%–3% level. This is less than our estimate of a 5.7% uncertainty on $L_{\rm bol}$.

Nevertheless, we consider the possibility that the absolute mid-IR flux may not be representative of the average or typical state of Gl 570D. If we relax the absolute flux calibration of the IRS spectrum, do we still see an NH_3 depletion? For this purpose, we have repeated the fitting procedure described in § 5.4 with the flux calibration adjusted by a factor that minimizes the value of χ^2. Allowing for the estimated noise in each pixel of the observed spectrum, we find that the nonequilibrium models always fit better than the equilibrium models at the $\sim$17 σ level, with insignificant variation between models A, B, and C.

6.5. *Photodissociation of* NH_3

NH_3 is a molecule that is easily dissociated by UV photons at $\sim$1900 Å. Since Gl 570D is a companion to a main-sequence star, it is possible that the UV flux from the primary results in a depletion of NH_3 in Gl 570D. This process was discussed in detail by Saumon et al. (2000) in the case of another late T dwarf with a companion, Gl 229B, where it was found to be completely negligible at the level of the photosphere. By comparison, the UV flux of the dK4 star Gl 570A is about 10 times larger than that of the dM1 star Gl 229A (based on the NextGen models of Allard & Hauschildt 1999), but the flux incident on Gl 570D is smaller because of the much greater projected separation (1525 AU [Burgasser et al. 2000] rather than 44 AU [Golimowski et al. 1998] for Gl 229B). Since the atmospheres of both brown dwarfs are quite similar, we can expect that the photodissociation of NH_3 in Gl 570D will be $10 \times (44/1525)^2$, $\sim$0.008 times that of Gl 229B. The Gl 570 BC pair of M dwarfs lies about 10 times closer to Gl 570A than Gl 570D, and their contribution to the UV flux incident on Gl 570D is a small correction to the above estimate.

7. CONCLUSION

Our method to determine $T_{\rm eff}$ and the gravity of brown dwarfs is most effective when applied to objects with known parallax that are members of systems where the primary provides the metallicity and age indicators. The method is based on integrated fluxes and evolution sequences rather than a direct fit of the spectrum, an approach that largely eliminates biases due to remaining systematic problems in the model spectra. With recalibrated optical and near-IR spectra and, most importantly, a *Spitzer* IRS spectrum, we have redetermined $T_{\rm eff}$ and g for Gl 570D to find nearly the same values as Geballe et al. (2001).

An excellent fit of the IRS spectrum can only be obtained if the NH_3 abundance is reduced by nearly 1 order of magnitude in the upper atmosphere. This is most readily explained by vertical mixing that drives the nitrogen chemistry away from chemical equilibrium (Lodders & Fegley 2002). We have considered several other possible explanations, but none of them are plausible.

We find that in late T dwarfs, the nonequilibrium N_2/NH_3 ratio generally does not depend on the efficiency of mixing in the atmosphere. Therefore, while the 10–11 μm band of NH_3 is a sensitive indicator of nonequilibrium chemistry in brown dwarf atmospheres, it provides little information about the efficiency of mixing. On the other hand, the CO abundance is very sensitive to the choice of the mixing parameter K, and photometric or spectroscopic observations of the 4.7 μm CO band are the most effective ways to determine K. Our study provides the most accurate parameters of any known brown dwarf (Fig. 1): $T_{\rm eff} = 800$–820 K, $\log g = 5.09$–5.23, $R = 0.0901$–0.0853 $R_\odot$, $\log L/L_\odot = -5.525$ to -5.551, $M/M_{\rm J} = 38$–47, and an age of 3–5 Gyr. The upper limit of this range (Fig. 1) is at least 2.8 σ more likely than the lower limit. Gl 570D joins Gl 229B as the second T dwarf where the effect of nonequilibrium chemistry due to vertical transport has been demonstrated explicitly.

This work is based (in part) on observations made with the *Spitzer Space Telescope*, which is operated by the Jet Propulsion Laboratory, California Institute of Technology, under NASA contract 1407. T. R. and M. M. acknowledge the support of the NASA Office of Space Sciences. K. L. is supported by NSF grant AST 04-06963. Part of this work was supported by the United States Department of Energy under contract W-7405-ENG-36, and NASA through the *Spitzer Space Telescope* Fellowship Program through a contract issued by the Jet Propulsion Laboratory, California Institute of Technology, under a contract with NASA. This research has benefited from the M, L, and T dwarf compendium housed at http://www.DwarfArchives.org and maintained by C. R. Gelino, J. D. Kirkpatrick, and A. J. Burgasser.

REFERENCES

Ackerman, A. S., & Marley, M. S. 2001, ApJ, 556, 872
Allard, F. Hauschildt, P. H., Alexander, D. R., Tamanai, A., & Schweitzer, A. 2001, ApJ, 556, 357
Angulo, C., et al. 1999, Nucl. Phys. A, 656, 3
Barshay, S. S., & Lewis, J. S. 1978, Icarus, 33, 593
Bézard, B., Lellouch, E., Strobel, D., Maillard, J.-P., & Drossart, P. 2002, Icarus, 159, 95
Burgasser, A. 2002, Ph.D. thesis, California Inst. of Technology

Burgasser, A. J., Geballe, T. R., Leggett, S. K., Kirkpatrick, J. D., & Golimowski, D. A. 2006, ApJ, 637, 1067
Burgasser, A. J., Kirkpatrick, J. D., Liebert, J., & Burrows, A. 2003, ApJ, 594, 510
Burgasser, A. J., et al. 2000, ApJ, 531, L57
Burrows, A., & Liebert, J. 1993, Rev. Mod. Phys., 65, 301
Burrows, A., Sudarsky, D., & Lunine, J. I. 2003, ApJ, 596, 587
Burrows, A., et al. 1997, ApJ, 491, 856
Chabrier, G., & Baraffe, I. 1997, A&A, 327, 1039
Champion, J. P., Loete, M., & Pierre, G. 1992, in Spectroscopy of the Earth's Atmosphere and the Interstellar Medium, ed. K. N. Rao & A. Weber (New York: Academic Press), 339
Cushing, M. C., et al. 2006, ApJ, in press (astro-ph/0605639)
Fegley, B., Jr., & Lodders, K. 1994, Icarus, 110, 117
———. 1996, ApJ, 472, L37
Fegley, B., Jr., & Prinn, R. G. 1985, ApJ, 299, 1067
Fortney, J. J., et al. 2006, ApJ, 642, 495
Geballe, T. R., Saumon, D., Leggett, S. K., Knapp, G. R., Marley, M. S., & Lodders, K. 2001, ApJ, 556, 373
Golimowski, D. A., Burrows, C. J., Kulkarni, S. R., Oppenheimer, B. R., & Brukardt, R. A. 1998, AJ, 115, 2579
Golimowski, D. A., et al. 2004, AJ, 127, 3516
Griffith, C. A., & Yelle, R. V. 1999, ApJ, 519, L85
Hauschildt, P. H., Allard, F., & Baron, E. 1999, ApJ, 512, 377
Husson, N., Bonnet, B., Scott, N. A., & Chedin, A. 1992, J. Quant. Spectrosc. Radiat. Transfer, 48, 509
Leggett, S. K., et al. 2002, ApJ, 564, 452
Lewis, J. S., & Prinn, R. G. 1980, ApJ, 238, 357
Lodders, K. 2003, ApJ, 591, 1220
Lodders, K., & Fegley, B., Jr. 1994, Icarus, 112, 368
———. 2002, Icarus, 155, 393
———. 2006, Astrophys. Update, in press (astro-ph/0601381)
Marley, M. S., Saumon, D., Guillot, T., Freedman, R. S., Hubbard, W. B., Burrows, A., & Lunine, J. I. 1996, Science, 272, 1919
Noll, K. S., Geballe, T. R., & Marley, M. S. 1997, ApJ, 489, L87
Patten, B. M., et al. 2006, ApJ, in press (astro-ph/0606432)
Perryman, M. A. C., et al. 1997, A&A, 323, L49
Roellig, T. L., et al, 2004, ApJS, 154, 418
Rothman, L. S., et al. 2005, J. Quant. Spectrosc. Radiat. Transfer, 96, 139
Santos, N. C., Israelian, G., Mayor, M. Bento, J. P., Almeida, P. C., Sousa, S. G., & Ecuvillon, A. 2005, A&A, 437, 1127
Saumon, D., Chabrier, G., & Van Horn, H. M. 1995, ApJS, 99, 713
Saumon, D., Geballe, T. R., Leggett, S. K., Marley, M. S., Freedman, R. S., Lodders, K., Fegley, B., Jr., & Sengupta, S. K. 2000, ApJ, 541, 374
Saumon, D., Marley, M. S., Lodders, K., & Freedman, R. S. 2003, in IAU Symp. 211, Brown Dwarfs, ed. E. Martín (San Francisco: ASP), 345
Smith, M. D. 1998, Icarus, 132, 176
Stephens, D. C., & Leggett, S. K. 2004, PASP, 116, 9
Thorén, P., & Feltzing, S. 2000, A&A, 363, 692
Tsuji, T. 1964, Ann. Tokyo Astron. Obs., 9, 1
Valenti, J. A., & Fisher, D. A. 2005, ApJS, 159, 141
Visscher, C., & Fegley, B., Jr. 2005, ApJ, 623, 1221
Yung, Y. L., Drew, W. A., Pinto, J. P., & Friel, R. R. 1988, Icarus, 73, 516